Early Myocardial Clearance Kinetics of Technetium-99m-Teboroxime Differentiate Normal and Flow-Restricted Canine Myocardium at Rest

Gerald Johnson III, David K. Glover, Connie B. Hebert and Robert D. Okada

Saint Francis Medical Research Institute of the University of Oklahoma Health Sciences Center, Tulsa, Oklahoma

Technetium-99m-teboroxime (CardioTec) is a promising new myocardial perfusion imaging agent. The purposes of this study were to define teboroxime clearance kinetics in normal and flow-restricted myocardium over a 1-hr period and to determine whether teboroxime kinetics are useful in detecting myocardial hypoperfusion. Accordingly, the circumflex arteries of 23 dogs were stenosed. By using miniature cadmium-telluride radiation detectors, myocardial teboroxime activities were continuously monitored in both the control and the stenosed zones. Myocardial clearance of teboroxime was modeled and found to be biexponential over 1 hr. A significant difference in myocardial clearance between the normal and stenosed zones ($t_{1/2}$ = 4.5 ± 0.9 min versus 10.2 ± 2.6 min, respectively; $p < 0.05$) was observed for the first exponential phase (the first 5 min following initial uptake), but not for the second exponential phase ($t_{1/2}$ = 160.7 ± 35.9 min versus 140.4 ± 27.4 min, respectively; p = ns). One hour fractional teboroxime blood clearance was 0.95 ± 0.03, with most of the clearance occurring during the first 4 min. Gamma camera images of excellent quality demonstrated an initial defect with significant quantitative differential clearance over 1 hr. Thus, there are two phases of myocardial teboroxime clearance. During the early exponential clearance phase, teboroxime kinetics at rest may be able to differentiate between normal and hypoperfused myocardium.

J Nucl Med 1993; 34:630–636

Thallium-201 has been widely used for the assessment of myocardial perfusion and the diagnosis of coronary artery disease. However, new imaging agents based on ^{99m}Tc have been developed with properties better suited for Anger gamma camera imaging due to the higher photopeak and shorter half-life of ^{99m}Tc compared to ^{201}Tl. Technetium-99m-teboroxime (CardioTec, Squibb Diagnostics, Princeton, NJ) is one of a new class of neutral boronic acid adducts of technetium dioxime complexes (*1*), which has the following favorable properties: rapid blood-pool clearance (*2,3*), high myocardial extraction (*3–6*) and rapid myocardial clearance kinetics from normal myocardium (*3,5,6*). Rapid clearance from normal myocardium makes multiple studies possible within a short period of time (*7,8*). An excellent correlation has been demonstrated between teboroxime and ^{201}Tl (*7,9–11*) and between teboroxime and coronary arteriography (*8,12,13*) in the diagnosis of abnormal versus normal myocardial perfusion. Our laboratory (*14*) and others (*15,16*) have reported decreased teboroxime clearance from flow-restricted myocardium following pharmacologic stress. However, teboroxime kinetics have not been well defined in flow-restricted myocardium at rest. Accordingly, the objectives of the present study were to determine whether teboroxime clearance kinetics can differentiate normal from flow restricted myocardium at rest and relate both myocardial clearances and flow ratios to serial planar images.

Received Aug. 26, 1992; revision accepted Dec. 2, 1992.

For reprints and correspondence contact: Gerald Johnson III, PhD, Saint Francis Medical Research Institute, 6465 South Yale, Suite 1010, Tulsa, OK 74136.

METHODS

Experimental Preparation

Twenty-five adult male mongrel dogs (mean weight 23.0 ± 0.4 kg, range 19–28 kg) were anesthetized with sodium pentobarbital (26 mg/kg) administered intravenously. Supplemental anesthestic was administered throughout the experiment as necessary. Animals were ventilated by a positive pressure respirator (Harvard Apparatus, South Natick, MA) with 95% oxygen. The heart was exposed via a left thoracotomy at the fifth intercostal space and suspended in a pericardial cradle. The left circumflex (LCx) coronary artery was then carefully dissected free near the origin and an electromagnetic flow probe (SP2202 Statham Blood Flowmeter, Gould Electronics, Dallas, TX) was placed around the artery. A snare occluder was loosely positioned distal to the electromagnetic flow probe. Mean or phasic arterial pressure, distal LCx pressure, left atrial pressure, lead II of the ECG, wall motion in both LAD and LCx zones and LCx flow were continuously monitored. Arterial blood was monitored for pH and partial pressure of carbon dioxide and oxygen. Two

additional dogs were fully instrumented but not stenosed and served as controls for imaging. A complete description of the instrumentation for hemodynamic recording was previously published (*17*).

Miniature Radiation Detectors

Miniature lead-shielded cadmium-telluride radiation detectors were positioned against the epicardium of the left ventricular anterior and posterior walls in close proximity to the sonomicrometer crystals and sutured in place. The physical characteristics of these detectors have been previously reported (*18*).

Preparation of Teboroxime

Kits for the preparation of teboroxime were supplied in a lyophilized form (Squibb Diagnostics, Princeton, NJ). A vial of teboroxime was reconstituted by the addition of 25 mCi of [^{99m}Tc]pertechnetate in accordance with instructions supplied by Squibb (*19*). Chromatographic results indicated that radiochemical purity was 94.0% ± 0.4%. Just prior to injection, a volume of the vial having 5 mCi of activity was withdrawn into a lead shielded syringe.

Gamma Camera Imaging

Images of the heart were obtained with a mobile scintillation camera (Model 420, Ohio-Nuclear Inc., Solon, OH) interfaced with a DPS 2800 nuclear imaging computer system (ADAC Laboratories, Milpitas, CA). A high-resolution collimator was used in conjunction with a 20% energy window encompassing the 140 keV ^{99m}Tc photopeak. Imaging was performed in the left lateral projection. Lead shielding was placed over the abdomen, under the heart and on both sides of the chest cavity of each dog to partially eliminate splanchnic activity and scatter. Dynamic images were collected in a 128 × 128 × 16 matrix with a 60-sec acquisition time for the first 10 min. Static images were collected in a 128 × 128 × 16 matrix with a 60-sec acquisition time at 15, 30 and 60 min.

Image quality was assessed quantitatively by using target-to-background (heart-to-lung) pixel-count ratios. Images were also quantified by calculating average pixel-count ratios in regions of interest (ROIs) in the control and flow-restricted myocardial zones. Regions of interest were defined as being three separate areas of 3 × 3 pixels each. These ROIs remained constant in size and location as images taken at several time points were analyzed.

Experimental Protocol

Figure 1 illustrates the experimental protocol. Baseline hemodynamic measurements were recorded during a 15-min period following instrumentation in 23 dogs which received stenoses. Varying degrees of LCx coronary artery stenosis were created by the partial occlusion of the artery with the snare occluder. The snare was adjusted until there was a reduction in resting flow and elimination of the reactive hyperemic response to a brief, total occlusion of the LCx. Two dogs that were fully instrumented but not subjected to stenosis served as controls for imaging purposes. Five millicuries of ^{99m}Tc-teboroxime was administered into the right femoral vein. A microsphere blood flow determination was made simultaneously by injecting 2–3 million 11 micron radiolabeled microspheres into the left atrium. The microspheres were labeled with either ^{113}Su, ^{103}Ru, ^{95}Nb or ^{46}Sc. The order in which the microspheres were injected was

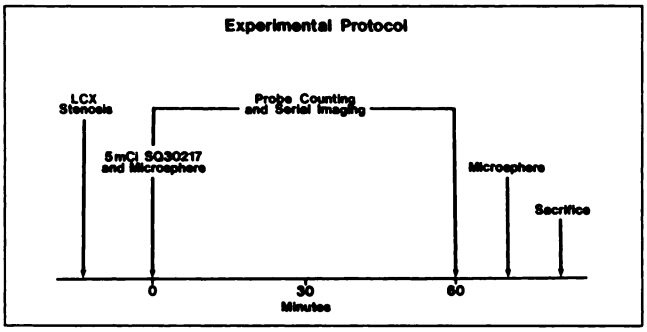

FIGURE 1. Experimental protocol. Following stenosis of the left circumflex coronary artery, teboroxime was injected and cadmium-telluride probe counting and planar imaging were begun immediately and continued for 1 hr. Microsphere blood flow determinations were made at the times shown.

randomized across experiments. Microsphere reference blood collection was begun 10 sec prior to each microsphere injection and continued for 2 min after injection. The microsphere technique has been used extensively in our laboratory and has been previously described (*20*). A thermodilution cardiac output determination was also made at this time.

Normal and ischemic zone regional myocardial ^{99m}Tc activities were continuously monitored over a 1-hr period using the miniature cadmium-telluride radiation detectors and recorded on a multichannel analyzer. Serial gamma camera images were also acquired during this period.

To measure blood ^{99m}Tc activity, 1.0-ml serial arterial blood samples were collected at 30-sec intervals during the first 2 min and then at 2-min intervals for 10 min. Samples were also collected at 20, 30 and 60 min postinjection. A final myocardial blood flow determination was made by injecting a second set of microspheres into the left atrium and a second cardiac output determination was made. The dogs were then killed.

Following death, the heart was quickly removed and the area of the myocardium from each zone was divided into 24 samples per zone and weighed (0.8–1.2 g/sample). Technetium-99m serial blood samples and myocardial tissue samples were counted in a gamma well counter (Model 1282, LKB Instruments, Gaithersburg, MD) with a window setting of 120–160 keV to detect ^{99m}Tc activity. These count data from the gamma counter were corrected for background and radioactive decay. Appropriate window settings were chosen for each microsphere isotope. Samples were corrected for both background and spillover of activity from one window into another and regional myocardial blood flows were calculated.

All experimental animals were handled in accordance with the *Position of the American Heart Association on Research Animal Use* and with the approval of the Institutional Animal Care and Use Committee of the University of Oklahoma Health Sciences Center.

Data Analysis

The first blood sample in each experiment was discarded because the activity of this sample was lower than that of the 30-sec sample due to inadequate time for complete mixing of teboroxime in the blood pool. Then background and decay-corrected serial blood sample data were normalized to the percent

TABLE 1
Hemodynamic Parameters

	Initial	Poststenosis	Final
MAP (mmHg)	104.9 ± 3.4	99.6 ± 3.2	100.0 ± 3.3
HR (bpm)	121.3 ± 3.6	113.9 ± 3.9	110.2 ± 4.0*
CO (liter/min)	2.3 ± 0.1	2.4 ± 0.1	2.1 ± 0.1
DP (mmHg)	101.7 ± 3.2	37.7 ± 2.6*	34.0 ± 1.8*
LAP (mmHg)	5.2 ± 0.6	6.9 ± 0.5*	6.3 ± 0.6

*$p < 0.05$ (from initial); mean ± s.e.m., n = 21.
MAP = mean arterial pressure; HR = heart rate; CO = cardiac output; DP = distal left circumflex coronary artery pressure; LAP = left atrial pressure.

activity at 30 sec and the individual activity versus time curves were modeled using a nonlinear regression analysis.

Myocardial clearance data were recorded from the cadmium-telluride probes at 1-min intervals and corrected for background and ^{99m}Tc decay. The first minute of data was omitted from further analysis due to potential added activity from the blood pool. The data for each zone were then normalized to the peak activity at 2 min in that zone. These individual myocardial zone data were summed across studies and every fifth minute of data was plotted. Decay- and background-corrected, non-normalized clearance data from both zones for each dog were modeled using nonlinear regression techniques in order to statistically compare myocardial clearance kinetic parameters between zones.

Fractional myocardial clearance was defined as the difference between the initial and final counts divided by the initial counts. It was calculated from the background- and decay-corrected, non-normalized data from the normal and stenosed zones for each dog beginning 2 min following teboroxime injection.

All results were expressed as mean ± 1 s.e.m. Each dog served as its own control. Comparisons across time were made using analysis of variance with repeated measures. Comparisons between normal and ischemic zones were made using paired t-tests. Pearson r correlation coefficients were calculated to assess the strength of relationships between variables. P values less than 0.05 were considered significant.

RESULTS

Hemodynamic Data

Complete hemodynamic data were obtained for 21 dogs and are presented in Table 1. Two dogs had incomplete data and were excluded from this analysis. The mean heart rate declined following stenosis with further decline at the end of the experiment. Baseline mean arterial blood pressure remained near 100 mmHg throughout the experiment. Distal LCx coronary artery pressure fell significantly poststenosis and remained until the end of the experiment. Mean left atrial pressure was elevated poststenosis and remained so until the end of the experiment. Cardiac output did not change significantly throughout the experiment. No changes in any hemodynamic parameters were noted as a result of teboroxime injection.

Regional Myocardial Function

The wall thickening fraction was calculated from sonomicrometer-determined end-systolic and end-diastolic wall thicknesses for each dog at the beginning, poststenosis and end of the experiment. The wall thickening fraction did not change significantly in the control zone (19.9 ± 1.4 beginning versus 20.2 ± 1.7 end) or the stenosis zone (16.6 ± 0.9 beginning versus 14.5 ± 1.0 end) during the 1-hr experimental period. Following stenosis, there was no significant difference between the normal and ischemic zones in the wall thickening fraction (20.9 ± 1.7 versus 17.0 ± 0.9, $p < 0.07$).

Myocardial Blood Flow

Regional myocardial blood flows were determined by radiolabeled microspheres and flow ratios were calculated. Blood flow in the ischemic zone was significantly reduced compared to the normal zone flow following stenosis (0.44 ± 0.06 versus 0.86 ± 0.04 ml/min/g, respectively; $p < 0.0001$) and remained so at the end of the study (0.37 ± 0.05 versus 0.78 ± 0.05; $p < 0.0001$). The mean ratio of the LCx coronary artery (stenosis zone) blood flow-to-LAD coronary artery (control zone) blood flow was 0.54 ± 0.05 following stenosis and 0.48 ± 0.05 at the end of the experiment (p = ns).

Myocardial Technetium-Teboroxime Distribution

The mean tissue technetium ratio (stenosis zone/control zone) at the end of the experiment was 0.82 ± 0.04. This value was significantly higher than the mean blood flow ratio determined by microspheres at the time of teboroxime administration (0.54 ± 0.05, $p < 0.0001$) and the mean blood flow ratio at the end of the experiment (0.48 ± 0.05, $p < 0.0001$). These results are indicative of differential clearance of teboroxime. The tissue technetium ratio was significantly correlated with the blood flow ratio at the time of teboroxime administration ($r = 0.88$, $p < 0.0000$, $n = 23$), indicating a substantial degree of dependence of the final tissue ratio on the initial blood flow ratio. Figure 2 illustrates the best fit regression line through a scatter plot of these data, all of which appear

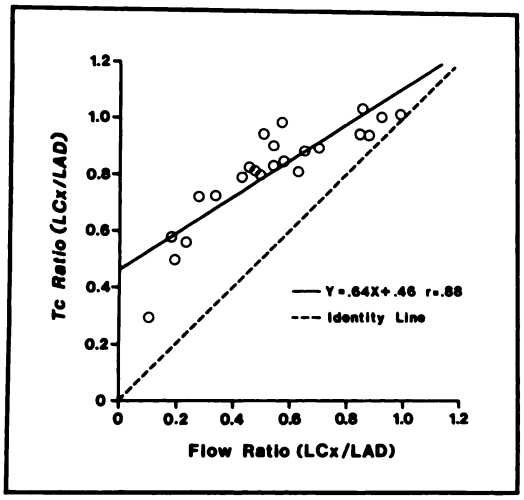

FIGURE 2. Final technetium ratio versus initial flow ratio. This scatter plot illustrates the relationship between flow at the time of teboroxime injection and final myocardial technetium distribution. The regression line through the data is shifted up and to the left of the line of identity, indicating differential clearance.

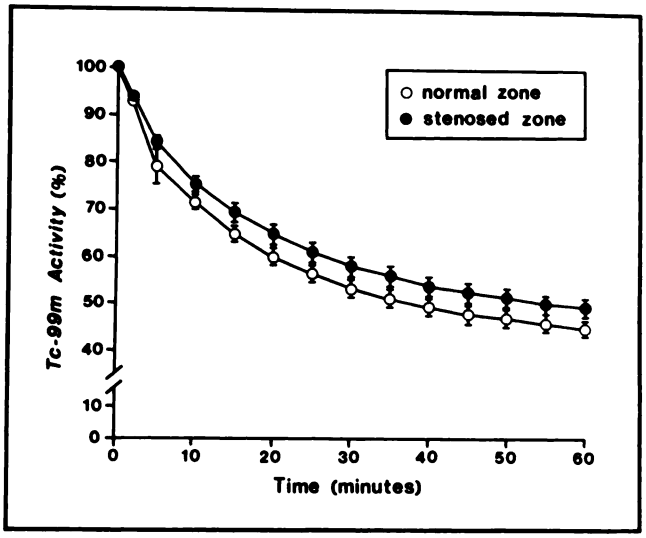

FIGURE 4. Regional myocardial clearance. Background and radioactive decay-corrected time versus activity curves for normal and ischemic myocardial zones with error bars. There was a similar pattern of teboroxime clearance from both myocardial zones consisting of a rapid early phase followed by a slow late phase.

above the line of identity and indicate differential myocardial clearance of teboroxime.

Myocardial and Blood Clearance Kinetics

Teboroxime blood clearance was triexponentially modeled and displayed in Figure 3. The modeled parameters were: $Y = 7.9 \times e(-0.007\ X) + 52.4 \times e(-13.7\ X) + 153.9 \times e(-0.958 \times X)$. There was a rapid initial component occurring during the first 4 min with 90% clearance in the first 10 min.

Figure 4 illustrates biexponential myocardial clearance consisting of an initial rapid phase followed by a slower second phase. Clearance is qualitatively seen to be slightly faster in the control zone in comparison to the flow-restricted zone. Figure 5 illustrates the mean fractional myocardial clearances at the end of 1 hr. Mean total fractional clearance from the control zone was 0.58 ± 0.02, while the mean total fractional clearance from the stenosis zone was 0.55 ± 0.02 (p = ns).

To quantitatively compare myocardial clearance kinetics between normal and flow-restricted zones, data from each dog were modeled using nonlinear regression techniques and found to be biexponential. The $t_{1/2}$ of the early

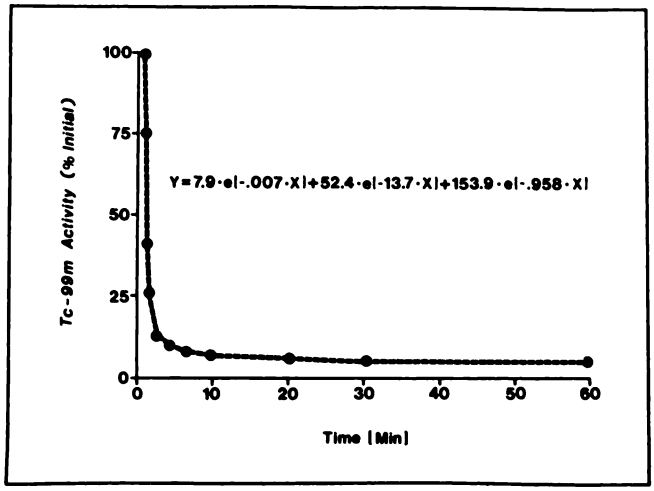

FIGURE 3. Blood clearance. This figure illustrates the mean teboroxime blood clearance over 1 hr obtained from serial arterial blood samples. Blood clearance was modeled using nonlinear regression techniques and was found to be triexponential.

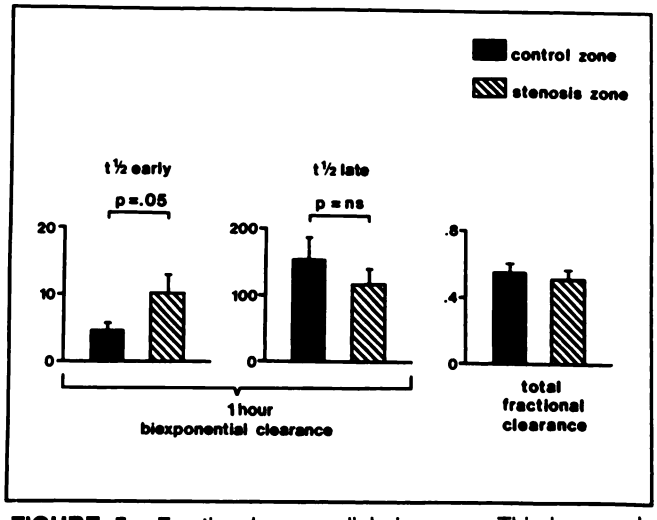

FIGURE 5. Fractional myocardial clearance. This bar graph displays the mean 1-hr fractional myocardial clearances with s.e.m. bars for the two myocardial zones. The half-time of the early phase was significantly longer (i.e., slower clearance) in the ischemic versus the normal zone. However, there were no significant differences between the control (filled bar) and the stenosis (striped bar) zones during the late phase.

phase was significantly longer (i.e., slower clearance) in the stenosis zone than in the control zone (10.2 ± 2.6 versus 4.5 ± 0.9 min, respectively, $p < 0.05$). During the late phase of 1 hr of myocardial clearance, the $t_{1/2}$ values for the two zones were not significantly different (140.4 ± 27.4 versus 160.7 ± 35.9 min).

Gamma Camera Images

Full sets of dynamic and static images were acquired for 23 dogs. Figure 6 illustrates the gamma camera images acquired initially at 5, 10, 15, 30 and 60 min after teboroxime administration from a control heart and a heart with LCx coronary artery stenosis. As can be seen in the figure, initial myocardial images were of excellent quality. Images at 60 min postinjection, acquired with comparable collection times, were of only fair quality due to low count statistics.

The upper panel in Figure 6 represents planar gamma camera images acquired from a dog that served as a control, while the lower panel illustrates the images from a dog in the stenosed group with a resting flow ratio of 0.64. A posterior wall perfusion defect is readily detectable on the initial images and persists 60 min later. Evidence of significant differential clearance in the images from the stenosed group was difficult to appreciate visually.

Quantitative image analysis was performed by forming pixel-count ratios from defined ROIs in the septal area (normal zone) and posterior wall (ischemic zone). Images were neither background-corrected nor decay-corrected. The ischemic-to-normal pixel count ratio at 2 min (0.65 ± 0.05) was significantly lower than that at both 10 min (0.72 ± 0.04; $p < 0.05$) and 60 min (0.80 ± 0.04; $p < 0.001$). Furthermore, the 10-min ratio was significantly lower than the 60-min ratio ($p < 0.01$), indicating significant defect fill-in.

Heart-to-lung pixel count ratios were obtained by defining ROIs in the target and background organs and comparing ratios from initial and final images. Heart-to-lung pixel-count ratios were significantly higher at the beginning of 1 hr of imaging than at the end of the study period (2.48 ± 0.1 versus 1.59 ± 0.06; $p < 0.05$).

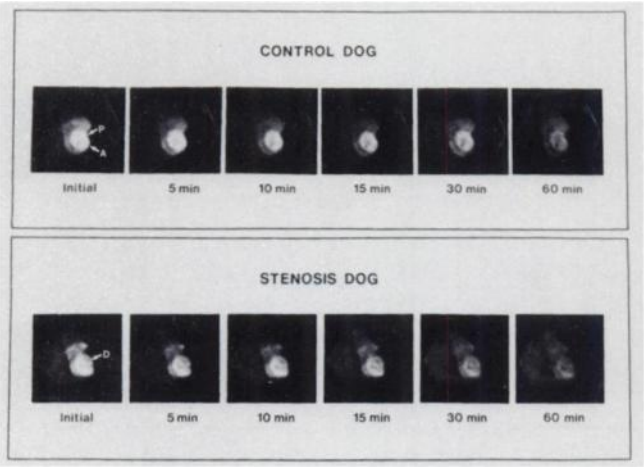

FIGURE 6. Gamma camera images. The upper panel shows serial planar images from a control dog, while the lower panel shows images from a dog with a left circumflex coronary artery stenosis. Note the prominent posterior wall perfusion defect and the absence of differential clearance over 1 hr. A = apex, D = defect and P = posterior wall.

DISCUSSION

The pattern of hemodynamic alterations observed is consistent with stenosis of a major coronary artery, i.e., significant reduction of coronary artery pressure distal to the stenosis and slight elevation of left atrial pressure. Teboroxime injection produced no observable hemodynamic changes during these experiments.

The comparison of wall thickening fraction in the normal and ischemic zones did not reach statistical significance in this study. However, the p value of 0.07 did indicate a trend towards significance. This is indicative of the heterogeneity of the stenosis group studied and reflects the fact that some flow restrictions did produce substantial alterations in wall motion, as would be expected. On average, the degree of stenosis achieved did not reduce flow sufficiently to significantly alter myocardial wall motion in this heterogeneous stenosis group.

Teboroxime blood clearance was rapid, with 90% of the radiotracer being cleared in the first 10 min which is in agreement with previous data from animal models (*3,15*). A triexponential model provided the best fit to these data.

Myocardial clearance was modeled and found to be biexponential with a rapid early phase followed by a slower late phase. Biexponential kinetics in normal myocardium under resting conditions have been reported by Stewart et al. (*5*) following either an intracoronary (*5*) or i.v. bolus injection (*15*) of teboroxime. Our quantitative data indicated that very early clearance kinetics, i.e., during the first 5 min, differentiate between normal and stenosed zones at rest, while later clearance kinetics did not. Therefore, it would appear that the greatest differences in clearance kinetics from the two myocardial zones occurred very early due to flow-related differences (*5*). Late clearance kinetics, which are apparently unrelated to flow, account for the parallel clearance curves which were not significantly different at 1 hr. Beanlands et al. (*21*) have recently shown that teboroxime retention is initially linear over a wide flow range. However, tracer retention subsequently underestimates flow changes at moderate to high flow rates after only 5 min.

The final gamma well counter determined tissue technetium ratio (stenosed/normal) was significantly greater than the microsphere determined blood flow ratio (stenosed/normal) at the time of teboroxime administration. This indicated the occurrence of differential clearance. The strong positive association between tissue techne-

tium ratio and blood flow ratio suggests that the final distribution of technetium in myocardium is primarily due to the effects of flow and to flow disparities between normal and stenosed regions. The finding that tissue technetium ratios are significantly correlated with stenosed zone flows but not with normal zone flows at the time teboroxime was injected indicates that it is the delay of the stenosed zone clearance, due to lower flow, which is primarily responsible for the final tissue technetium ratio. Pieri et al. (*22*) also found a strong correlation between regional myocardial perfusion measured with microspheres and teboroxime activity ratio (abnormal/normal) derived from images. Thus, quantitative information from serial planar images confirmed evidence from the miniature cadmium-telluride probes and gamma well counter.

We calculated pixel-count ratios (stenosed zone/normal zone) on serial planar images acquired at 2, 10 and 60 min for each dog in the study. We found that the 2-min pixel-count ratio was significantly lower than that at both 10 and 60 min, which provides quantitative evidence of differential clearance. Other investigators using exercise or pharmacologic stress studies (*7,9,12,15,23,24*) have supported the concept of early differential clearance by suggesting that imaging within 5 min of injection is required to detect flow disparities before differential clearance of teboroxime reduced these disparities.

Qualitatively interpreted serial planar images did reveal defects in the zone served by the stenosed vessel compared to normal zones. However, visual evidence of differential clearance was not always present. This is not surprising since a range of stenosis severity was obtained. It is possible that the amount of differential clearance was too small to be discernible by qualitative analysis based on gamma camera images, i.e., less than 25%. The use of computers and mathematical algorithms in the clinical setting to provide quantitative assessment of images could allow increased ability to identify hypoperfused areas at rest which are not apparent by qualitative analysis alone.

Either the addition of dipyridamole or adenosine prior to imaging or the use of an exercise/rest protocol would allow maximal opportunity to view such differential clearance in the presence of stenosis. In a clinical stress/rest double injection study, Hendel et al. (*7*) found that 9 of 14 abnormal studies demonstrated early differential clearance. They observed rapid differential clearance of teboroxime, including the disappearance of defects on post-exercise images. They reported differential clearance of teboroxime, similar to thallium differential clearance, but with a much shorter time course, i.e., within the first 5 min.

LIMITATIONS

Binding of teboroxime to red blood cells and plasma proteins has been shown to decrease myocardial extraction in an isolated perfused rat heart preparation (*25*). The extent to which this binding may affect clearance kinetics in a dog model is unknown. We did not measure or control binding in these experiments.

We used hepatic shielding in these studies which probably improved image quality. In clinical imaging studies, derivation of quantitative kinetic data from the inferior wall may be more problematic.

Introduction of sampling error was possible when ROIs were placed on images where we did not attempt to sample the entire area subserved by the LAD or LCx. However, care was taken in placing these ROIs in order to avoid contamination with the blood pool and surrounding tissue.

In the present study, the extent of redistribution demonstrated by probes was less than that by well counting. We feel that this is due to the inability to measure probe counts during the first minute postinjection due to high blood-pool activity from the bolus. As our data demonstrate, most of the redistribution occurs during the first minutes after tracer administration.

CLINICAL SIGNIFICANCE

The current study demonstrated differential clearance and redistribution in a canine model of resting hypoperfusion. These data add to our basic knowledge of teboroxime kinetics. Clinically, these data may have potential applicability, since most exercise or pharmalogic stress studies also involve a separate rest injection image. Furthermore, rest teboroxime imaging has been proposed to assess myocardial area at risk prior to reperfusion therapy and in conjunction with stress sestamibi imaging.

Data from this study and others (*7,9,14,16*) have shown that imaging of teboroxime must begin soon after injection due to the rapid myocardial uptake and clearance kinetics of this agent. Blood-pool clearance is also quite rapid, thus permitting commencement of imaging within minutes of injection. Our findings indicate that the greatest difference in myocardial clearance kinetics between stenosed and normal zones occurs very early and therefore differential clearance could be missed when imaging does not start early. However, these small differences in clearance, representing redistribution, were not always detectable qualitatively and will require improved quantitative image analysis techniques in order to achieve clinical utility.

CONCLUSIONS

Regional probe data have shown that teboroxime myocardial clearance kinetics are rapid and can distinguish hypoperfused from normal myocardium at rest. Quantitative imaging data were also presented that support the concept of rapid differential myocardial clearance of teboroxime.

ACKNOWLEDGMENTS

The authors thank Squibb Diagnostics for their continued support of this investigation and Kiem N. Nguyen for excellent assistance in graphic arts production.

REFERENCES

1. Treher EN, Gougoutas J, Malley M, Nunn AD, Unger SE. New technetium radiopharmaceuticals boronic acid adducts of vicinal dioxime complexes. *J Lab Compd Radiopharm* 1986;23:1118–1120.
2. Narra RK, Feld T, Wedeking P, Matyas J, Nunn AD, Coleman RE. SQ30217, a technetium-99m labeled myocardial imaging agent which shows no interspecies differences in uptake. *Nuklearmedizin* 1987; 23(suppl):489–491.
3. Narra RK, Nunn AD, Kuczynski BL, Feld T, Wedeking P, Eckelman WC. A neutral technetium-99m complex for myocardial imaging. *J Nucl Med* 1989;30:1830–1837.
4. Leppo JA, Meerdink DJ. Comparative myocardial extraction of two technetium-labeled BATO derivatives (SQ30217, SQ30214) and thallium. *J Nucl Med* 1990;31:67–74.
5. Stewart RE, Schwaiger M, Hutchins GD, et al. Myocardial clearance kinetics of technetium-99m-SQ30217: a marker of regional myocardial blood flow. *J Nucl Med* 1990;31:1183–1190.
6. Marshall RC, Leidholdt EM Jr, Zhang D-Y, Barnett CA. The effect of flow on technetium-99m-teboroxime (SQ30217) and thallium-201 extraction and retention in rabbit heart. *J Nucl Med* 1991;32:1979–1988.
7. Hendel RC, McSherry B, Karimeddini M, Leppo JA. Diagnostic value of a new myocardial perfusion agent, teboroxime (SQ30217), utilizing a rapid planar imaging protocol: preliminary results. *J Am Coll Cardiol* 1990;16: 855–861.
8. Seldin DW, Johnson LL, Blood DK, et al. Myocardial perfusion imaging with technetium-99m SQ30217: comparison with thallium-201 and coronary anatomy. *J Nucl Med* 1989;30:312–319.
9. Iskandrian AS, Heo J, Nguyen T, Mercuro J. Myocardial imaging with Tc-99m teboroxime: technique and initial results. *Am Heart J* 1991;121: 889–894.
10. Labonte C, Taillefer R, Lambert R, et al. Comparison between technetium-99m-teboroxime and thallium-201 dipyridamole planar myocardial perfusion imaging in detection of coronary artery disease. *Am J Cardiol* 1992;69:90–96.
11. Bontemps L, Geronicola-Trapali X, Sayegh Y, Delmas O, Itti R, Andre-Fouet X. Technetium-99m teboroxime scintigraphy. *Eur J Nucl Med* 1991;18:732–739.
12. Fleming RM, Kirkeeide RL, Taegtmeyer H, et al. Comparison of technetium-99m teboroxime tomography with automated quantitative coronary arteriography and thallium-201 tomographic imaging. *J Am Coll Cardiol* 1991;17:1297–1302.
13. Drane WE, Keim S, Strickland P, Tineo A, Nicole M. Preliminary report of SPECT imaging with technetium-99m teboroxime in ischemic heart disease. *Clin Nucl Med* 1992;17:215–225.
14. Johnson G III, Okada RD, Hebert C. Myocardial kinetics of technetium-99m teboroxime in a canine stenosis model following dipridamole [Abstract]. *J Nucl Med* 1991;32:948.
15. Stewart RE, Heyl B, O'Rourke RA, Blumhardt R, Miller DD. Demonstration of differential post-stenotic myocardial technetium-99m-teboroxime clearance kinetics after experimental ischemia and hyperemic stress. *J Nucl Med* 1991;32:2000–2008.
16. Gray WA, Gewirtz H. Comparison of technetium-99m teboroxime with thallium for myocardial imaging in the presence of a coronary artery stenosis. *Circulation* 1991;84:1796–1807.
17. Glover DK, Okada RD. Myocardial kinetics of technetium-MIBI in canine myocardium after dipyridamole. *Circulation* 1990;81:628–637.
18. Jacobs ML, Okada RD, Daggett WM, et al. Regional myocardial radiotracer kinetics in dogs using miniature radiation detectors. *Am J Physiol* 1982;242:H849–H854.
19. Squibb (CardioTec) package insert, Squibb Diagnostics, Princeton, NJ.
20. Domenech RJ, Hoffman JIE, Noble MIM, Saunders KB, Henson JR, Subijanto S. Total and regional coronary blood flow measured by radioactive microspheres in conscious and anesthetized dogs. *Circ Res* 1969; 25:581–596.
21. Beanlands R, Muzik O, Nguyen N, Petry N, Schwaiger M. The relationship between myocardial retention of technetium-99m teboroxime and myocardial blood flow. *J Am Coll Cardiol* 1992;20:712–719.
22. Pieri P, Yasuda T, Fischman AJ, et al. Myocardial accumulation and clearance of technetium-99m-teboroxime at 100%, 75%, 50% and zero coronary blood flow in dogs. *J Nucl Med* 1991;18:725–731.
23. Li QS, Solot G, Frank TL, Wagner HN Jr, Becker LC. Tomographic myocardial perfusion imaging with technetium-99m-teboroxime at rest and after dipyridamole. *J Nucl Med* 1991;32:1968–1976.
24. Nakajima K, Taki J, Bunko H, et al. Dynamic acquisition with a three-headed SPECT system: application to technetium-99m-SQ30217 myocardial imaging. *J Nucl Med* 1991;32:1273–1277.
25. Rumsey WL, Rosenspire KC, Nunn AD. Myocardial extraction of teboroxime: effects of teboroxime interaction with blood. *J Nucl Med* 1992;33:94–101.